Influence of the Process for Obtaining Massive Amorphous Materials on the Defects of the Structure in the Alloy $Fe_{61+x}Co_{10-x}Y_8W_1B_{20}$, where x = 0 or 1

MARCIN NABIALEK, BARTLOMIEJ JEZ*, KINGA JEZ
Institute of Physics, Faculty of Production Engineering and Materials Technology, Czestochowa University of Technology, 19 Armii Krajowej Str., 42-200 Czestochowa, Poland

As part of the work, a rapid cooled alloy was produced with the chemical composition $Fe_{61+x}Co_{10-x}Y_8W_1B_{20}$, where: x = 0 or 1 using two methods, suction in and injecting the molten alloy into the copper mold. The material was obtained in the form of 10 mm x 5 mm x 0.5 mm plates. Studies on the structure of the obtained alloys were carried out using X-ray diffraction. Obtained X-ray diffraction images are typical for amorphous materials. Using the vibration magnetometer, static magnetic hysteresis loops and primary magnetization curves were measured. The produced samples are characterized by a saturation value above 1T and a coercive field value below 200 A/m. Based on the theory of H. Kronmüller, numerical analysis of the curves of the original magnetization was carried out. It has been found that the process of magnetizing the produced materials has defects of the amorphous structure in the form of pseudo-location dipoles and free volumes. In addition, the spin wave stiffness parameter was determined.

Keywords**:** *amorphous alloy, chemical composition, defects, static magnetic hysteresis, X-ray diffraction*

Amorphous materials due to their different properties than their crystalline counterparts are an interesting object of research [1-3]. The most well-known methods for producing amorphous materials are cooling the liquid alloy at a sufficiently high speed. A well-known and widely used method is the casting of a liquid alloy on a rotating copper cylinder (cooling rate of 10^6K/s) [4, 5]. These materials are produced in the form of tapes with a thickness of less than 100 ìm, which significantly impairs their practical application. The answer to the limited application capabilities of thin strips and layers are massive amorphous materials [6-16]. These materials are produced by cooling the liquid alloy but at a much lower speed, in the range of 10^{-1}-10^3 K/sec. Applying three empirical criteria proposed by A. Inoue, it is possible to produce materials with an amorphous structure of a thickness exceeding several centimeters. Negative heat of mixing, multi-componentity of the alloy and correspondingly large differences in the length of atomic rays significantly hamper the process of diffusion of atoms over distances in the volume of the cooled alloy. The restriction of diffusion allows the disordered long-range atoms to remain in the material volume. This disorder determines the unique properties of amorphous materials. Depending on the chemical composition of the alloy, the amorphous materials exhibit the so-called soft magnetic properties such as the low coercivity field, high saturation magnetization or low loss [17-20]. The defects of the structure have a significant influence on the properties of amorphous materials. They take a similar form and fulfill similar roles as defects occurring in crystalline materials. Structural defects found in the volume of amorphous materials are divided into point defects and linear defects, so-called pseudo-location dipoles [21]. The presence of these defects is possible to detect by thoroughly analyzing the process of magnetizing the material sample. According to H. Kronmuller's theory, these defects affect the course of the magnetization curve [22, 23]. Apart from the influence of internal fluctuations, such as density anisotropy, magnetization near an area called the approach to ferromagnetic saturation can be defined as:

$$\mu_0 M(H) = \mu_0 M_s \left[1 - \frac{a_{1/2}}{(\mu_0 H)^{1/2}} - \frac{a_1}{(\mu_0 H)^1} - \frac{a_2}{(\mu_0 H)^2}\right] + b(\mu_0 H)^{1/2} \quad (1)$$

where: M_s-spontaneous magnetization, μ_0 -magnetic permeability of vacuum, H- magnetic field, a_i (i = 1/2, 1, 2) -angular coefficients of the linear fit, which correspond to the free volume and linear defects, b -slope of the linear fit corresponding to the thermally induced suppression of spin waves by a magnetic field of high intensity.

The factors in equation 1 can be described as follows:

$$\frac{a_{1/2}}{(\mu_0 H)^{1/2}} = \mu_0 \frac{3}{20 A_{ex}} \left(\frac{1+r}{1-r}\right)^2 G^2 \lambda_s^2 (\Delta V)^2 N \left(\frac{2A_{ex}}{\mu_0 M_s}\right)^{1/2} \frac{1}{(\mu_0 H)^{1/2}} \quad (2)$$

$$\frac{a_1}{\mu_0 H} = 1{,}1\mu_0 \frac{G^2 \lambda_s^2}{(1-\nu)^2} \frac{Nb_{eff}}{M_s A_{ex}} D_{dip}^2 \frac{1}{\mu_0 H} \quad (3)$$

$$\frac{a_2}{\mu_0 H^2} = 0{,}456\mu_0 \frac{G^2 \lambda_s^2}{(1-\nu)^2} \frac{Nb_{eff}}{M_s^2} D_{dip}^2 \frac{1}{(\mu_0 H)^2} \quad (4)$$

where: ΔV - means the change in volume due to the occurrence of a point defect characterized by a bulk density of N, A_{ex}-exchange constant, G - transverse elastic shear modulus, r-Poisson's ratio, λ_s -magnetostriction constant, D_{dip}- dlugosc defektu liniowego, l_H - odleglosc wymiany.

Equations (2-4) describe the effect of structural defects on the magnetization process. Equation (2) describes the effect of point defects, while the remaining equations relate to the influence of pseudo-dislocation dipoles for assumptions: $D_{dip} < 1_H$ (3) and $D_{dip} > 1_H$ (4). For the equation (4), l_H is the distance of at least two dipoles [24].

Above the area called the approach to ferromagnetic saturation magnetizing is associated with the suppression of thermally excited spin waves (Holstein-Primakoff paraproces [25]). The stiffness of the spin wave D_{spf} is

* *email: bartek199.91@o2.pl*

related to the parameter b, which can be described by the relationship:

$$b = 3{,}54 g\mu_0\mu_B \left(\frac{1}{4\pi D_{spf}}\right)^{3/2} kT(g\mu_B)^{1/2} \qquad (5)$$

where: k -Boltzman's constant, μ_B -Bohr magneton,
g- gyromagnetic factor.

The aim of the work was to determine the type of defects occurring in the amorphous structure of the alloy with the chemical composition $Fe_{61+x}Co_{10-x}Y_8W_1B_{20}$ where x = 0 or 1 based on the theory of H. Kronmuller. In addition, an attempt was made to determine the impact of the method of producing massive amorphous materials on the type and amount of structural defects.

Experimental part

The batch material was made using an arc furnace. Chemical elements with a purity above 99.99% were used. Samples weighing 5 grams with an accuracy of 0.001 grams were weighed. The material solidification process was carried out in a protective atmosphere of argon. Each time prior to remelting the batch, pure titanium was melted, which ensures a higher degree of cleanliness of the working chamber. The melting of the batch material was carried out at the current intensity in the range of 180-380 A. Before each subsequent remelting, the ingots were turned over to the other side using a manipulator to better mix the alloy constituents. The polycrystalline ingot obtained in this way was cleaned and crushed to smaller elements.

Two methods were used to create amorphous materials: injection molding and suction. These methods have similar cooling rates in the range of 10^1-10^3 K/s. The production process of amorphous material by these methods is similar. In both methods, a high vacuum was created in the working chamber. The casting of the molten alloy into the copper mold takes place under the protective gas conditions - argon. For both methods, the same protective gas pressure, 0.7 atmosphere was used. The alloy was cast into identical copper molds. The material was made in the form of 0.5 mm thick plates. In the suction method before melting of the batch, pure titanium was melted, in the injection method this process was not carried out due to technological reasons. During the production of amorphous materials by suction the charge is melted with a plasma arc, whereas in the case of the injection method the material is melted by means of so-called eddy currents. Another difference between these production methods is the direction of force: suction, or injection of a liquid alloy.

The structure of the produced materials was examined using X-ray diffraction in the 2 theta angle range from 30 to 100°. The BRUCKER X-ray diffractometer model Advanced 8 equipped with a CuK a lamp was used for powdered samples. Using the LakeShore vibration magnetometer, the original magnetizing curves and static loops of the magnetic histeresis were measured. The measurement was carried out in the magnetic field induction up to 1.7 T. The obtained primary curves of magnetization were subjected to numerical analysis in accordance with the theory of H. Kronmuller.

Results and discussions

The figure 1 presents X-ray diffractograms made for the prepared $Fe_{61}Co_{10}Y_8W_1B_{20}$ and $Fe_{62}Co_9Y_8W_1B_{20}$ alloys produced in two methods.

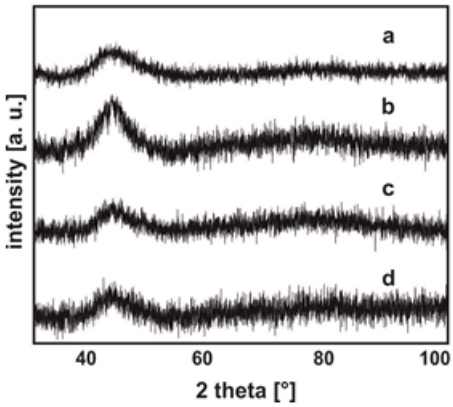

Fig.1. X-ray diffractograms for alloy samples produced by injection molding: a) $Fe_{61}Co_{10}Y_8W_1B_{20}$, b) $Fe_{62}Co_9Y_8W_1B_{20}$ and by suction: c) $Fe_{61}Co_{10}Y_8W_1B_{20}$, d) $Fe_{62}Co_9Y_8W_1B_{20}$

One wide maximum in the angle range two theta from 35 to 55° is visible on registered diffraction patterns. The occurrence of this maximum indicates an amorphous structure for the produced samples. This maximum comes from X-rays reflected from the chaotically distributed atoms in the volume of the samples tested. Figure 2 presents static magnetic hysteresis loops for manufactured alloy samples.

The measurement was carried out in the field of magnetic field induction from 0 to 1.7 T. Static hysteresis loops indicate the lack of magnetically hard phases in the volume of the tested samples. The manufactured alloys are characterized by a saturation magnetization greater than 1 T and a coercive field well below 1000 A/m which situates these materials in the group of so-called soft

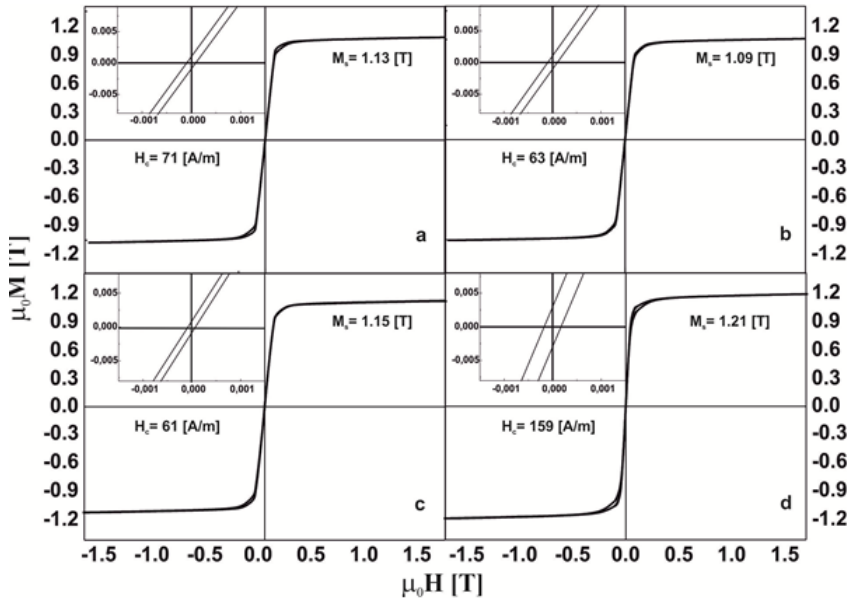

Fig.2. Static magnetic hysteresis loops with the enlarged center of the M-H system for alloy samples manufactured by injection molding: a) $Fe_{61}Co_{10}Y_8W_1B_{20}$, b) $Fe_{62}Co_9Y_8W_1B_{20}$ and by suction: c) $Fe_{61}Co_{10}Y_8W_1B_{20}$, d) $Fe_{62}Co_9Y_8W_1B_{20}$

magnetic materials [26]. Figure 3 presents the original magnetization curves for the samples produced.

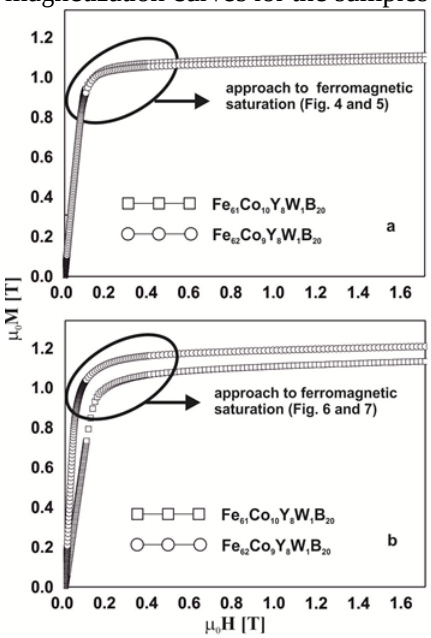

Fig. 3. Primary magnetization curves for $Fe_{61+x}Co_{10-x}Y_8W_1B_{20}$ alloy samples manufactured by: a) injection, b) suction

For the registered curves of the original magnetization, an area called the approach to ferromagnetic saturation was pre-determined. The curves were subjected to numerical analysis in accordance with the theory of H. Kronmüller (fig. 4-7)

The $Fe_{61}Co_{10}Y_8W_1B_{20}$ alloy produced by the injection method has both point and linear defects of the structure. In the field of magnetic field induction 0.063 - 0.089 T, the process of magnetizing the sample is related to the presence of free volumes. In the range 0.09 - 0.4 T, the dominant influence on the magnetization of the material has pseudo-location dipoles in accordance with the relations (3) and (4). Above the magnetic field induction 0.4 T, the magnetizing process is associated with the attenuation of thermally excited spin waves. Figure 5 presents the analysis of the primary curve for the $Fe_{61}Co_{10}Y_8W_1B_{20}$ alloy produced by injection molding. In this case, no influence of free volumes on the magnetizing process was noted. In the field of magnetic field induction 0.085 - 0.4 T, sample magnetization is based on the rotation of the magnetization vector near the line defects for which the dependences $D_{dip} < 1_H$ (0.09 - 0.16 T) and $D_{dip} > 1_H$ (0.16 - 0.4 T) are fulfilled. Similar to the $Fe_{62}Co_9Y_8W_1B_{20}$ alloy, the Holstein-Primakoff paraprocesses dominate in the magnetization process for the induction of a magnetic field above 0.4 T.

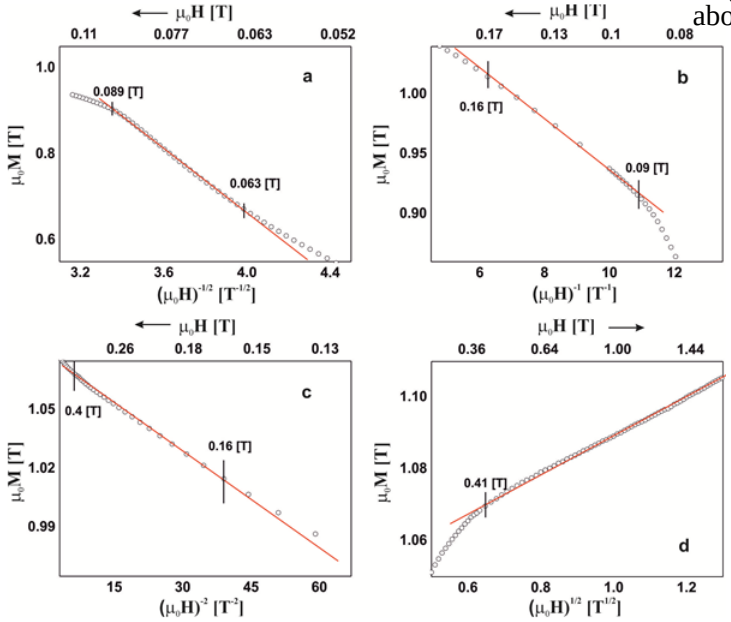

Fig.4. High-feld magnetic polarization curves as a function of $(\mu_0H)^{-1/2}$, $(\mu_0H)^{-1}$, $(\mu_0H)^{-2}$ and $(\mu_0H)^{1/2}$ for $Fe_{61}Co_{10}Y_8W_1B_{20}$ alloy made by injection method

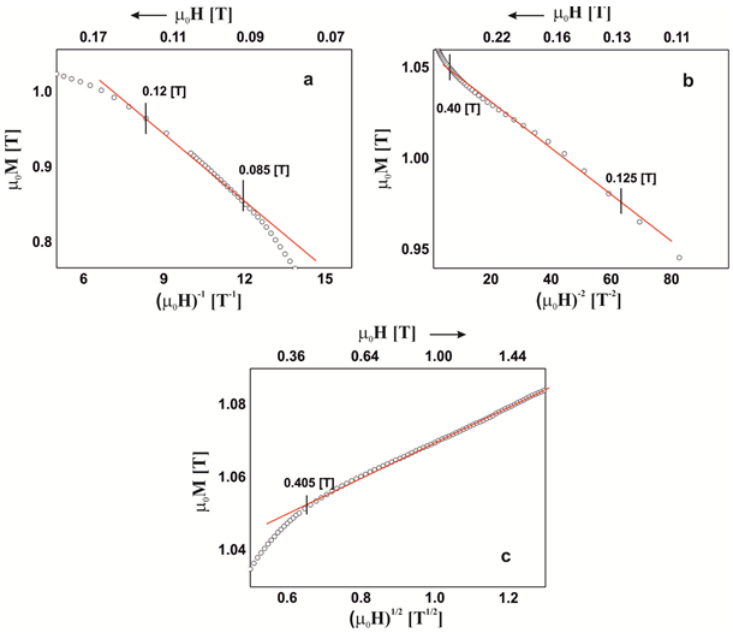

Fig.5. High-feld magnetic polarization curves as a function of $(\mu_0H)^{-1}$, $(\mu_0H)^{-2}$ and $(\mu_0H)^{1/2}$ for $Fe_{62}Co_9Y_8W_1B_{20}$ alloy made by injection method

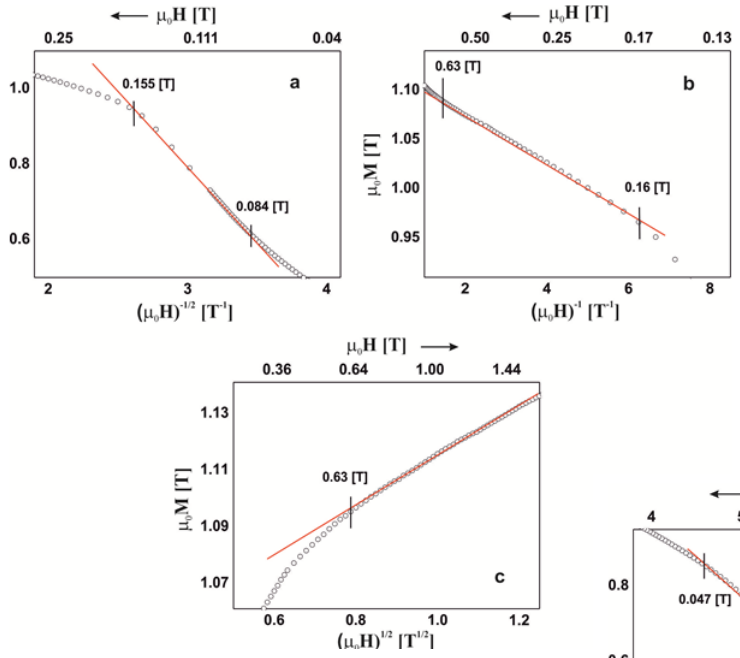

Fig.6. High-feld magnetic polarization curves as a function of $(\mu_0H)^{-1/2}$, $(\mu_0H)^{-1}$ and $(\mu_0H)^{1/2}$ for $Fe_{61}Co_{10}Y_8W_1B_{20}$ alloy made by suction method

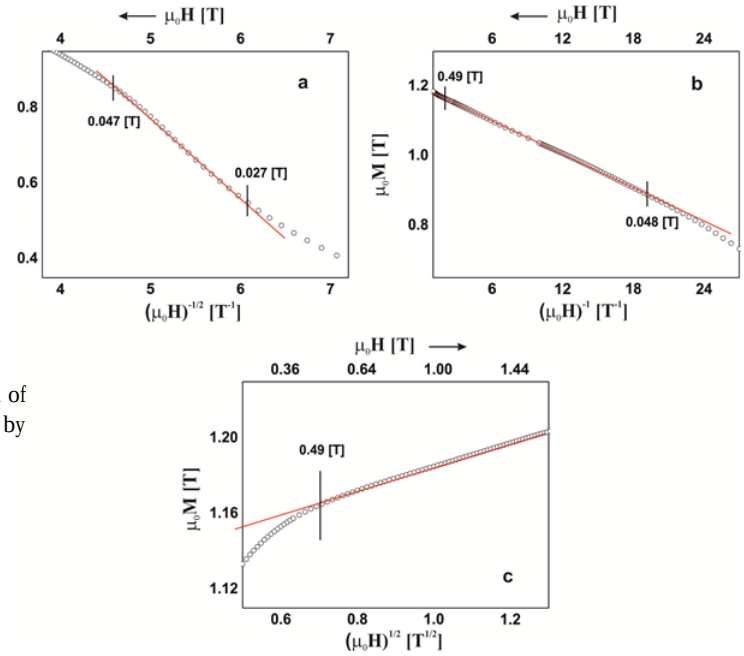

Fig.7. High-feld magnetic polarization curves as a function of $(\mu_0H)^{-1/2}$, $(\mu_0H)^{-1}$ and $(\mu_0H)^{1/2}$ for $Fe_{62}Co_9Y_8W_1B_{20}$ alloy made by suction method

Figure 6 presents the analysis of the primary magnetization curves for the $Fe_{61}Co_{10}Y_8W_1B_{20}$ alloy produced by suction. The process of magnetizing the sample of this alloy is associated with the presence of free volumes and pseudo-dislocation dipoles. However, in this case, the linear defects are characterized by dimensions smaller than the exchange distance l_H, according to the relationship (3). Holstein-Primakoff paraproces for the magnetic field starts around 0.63 T. In the same way, the process of magnetizing the $Fe_{62}Co_9Y_8W_1B_{20}$ alloy sample produced by suction takes place. Also in this case, the process of magnetizing the sample is associated with the presence of point and rope defects not exceeding the dimension of the exchange distance (table 1). The process of attenuation of thermally excited spin waves occurs in the induction of a magnetic field above 0.4 T.

Analyzing the determined values, it can be concluded that in the case of the alloys formed, a correlation between the value of the D_{spf} coefficient and magnetization of saturation takes place. It is assumed that the spin wave stiffness parameter is related to the surrounding of magnetic atoms by other magnetic atoms. Due to the chemical composition of the alloys produced, these are Fe-Fe, Fe-Co and Co-Co interactions. It should be expected that the higher value of saturation magnetization for alloys produced by the suction method should be associated with a higher value of D_{spf} and this is not the case. It is possible that the distances between magnetic atoms in certain areas of the sample are so small that the antiferromagnetic ordering becomes more privileged in terms of energy, which reduces the saturation of the material produced [27].

Table 1

DETERMINED MAGNETIC PROPERTIES FOR THE ALLOY $Fe_{61}Co_{10}Y_8W_1B_{20}$

Production method	Composition	μ_0M_s [T]	Dspf [meVnm^2]	H_c [A/m]	Point defects	Linear defects	
						$D_{dip}<l_H$	$D_{dip}>l_H$
injection	$Fe_{61}Co_{10}Y_8W_1B_{20}$	1.13	46.5	71	+	+	+
	$Fe_{62}Co_9Y_8W_1B_{20}$	1.09	55.9	63	-	+	+
suction	$Fe_{61}Co_{10}Y_8W_1B_{20}$	1.15	33.3	61	+	+	-
	$Fe_{62}Co_9Y_8W_1B_{20}$	1.21	42.4	159	+	+	-

Conclusions

The results obtained by the authors confirm the following conclusions:

The massive amorphous $Fe_{61+x}Co_{10-x}Y_8W_1B_{20}$ alloy is characterized by the so-called magnetically soft properties. The produced materials had a relatively high saturation magnetization value of about 1.1 T and a relatively low coercive field value below 150 A/m.

The research of the area called the approach to ferromagnetic saturation showed that the process of magnetizing the produced materials is related to the occurrence of both point and linear defects of the structure.

A clear influence of the production method on the resulting defects of $Fe_{61+x}Co_{10-x}Y_8W_1B_{20}$ alloy structure is visible. Samples produced using the suction method had linear structural defects in the form of pseudo-location dipoles, whose dimensions did not exceed the distance $D_{dip} << l_H$.

The alloys produced by the suction method were characterized by a higher saturation magnetization in comparison to alloys produced by the injection method.

The value of the D_{spf} parameter related to the distances between magnetic atoms achieves lower values for alloys produced by suction.

The increase in saturation magnetization with a simultaneous decrease in the D_{spf} parameter value can be linked to the antiferromagnetic ordering occurring for the samples of alloys produced by the injection method.

The method of introducing a liquid alloy affects the structure of the obtained materials. This is indicated by the different dimensions of linear structure defects and the various saturation values and the spin wave stiffness parameter depending on the production method.

References

1.INOUE, A., YANO, N., MASUMOTO, T., J. Mater. Science, **19**, 1984, p. 3786.

2.MCHENRY, M.E., WILLARD, M.A., LAUGHLIN, D.E., Prog. Mater. Sci., **44**, 1999, p. 291.

3.SZOTA, M., Archives of Metallurgy and Materials, **62**, no. 1, 2017 p. 217.

4.CHEN, H.S., MILLER, C.E., Review of Scientific Instruments, **41**, 1970, p. 12376.

5.KLEMENT, W., WILLENS, R.H., DUWEZ, P., Nature, **187**, 1960, p. 869.

6.INOUE, A., KATO, A., ZHANG, T., KIM, S.G., MASUMOTO, T., Materials Transaction JIM, **32**, 1991, p. 609.

7.TREXLER, M.M., THADHANI, N. N., Progress in Materials Science, **55**, 2010, p. 759.

8.JIAJIA, S., CHENXI, D., TAN, W., YIDONG, W., RONGSHAN, W., XIDONG, H., Journal of Alloys and Compounds, **741**, 2018, p. 542.

9.NABIALEK, M., BLOCH, K., SZOTA, M., SANDU, A.V., Materiale Plastice, **54,** no. 3, 2017, p. 491.

10.BLOCH, K., TITU, M.A., SANDU, A.V., Rev. Chim. (Bucharest), **68,** no. 9, 2017, p. 2162.

11.GRUSZKA, K., NABIALEK, M., SZOTA, M., VIZUREANU, P., ABDULLAH, M.M.A., BLOCH, K., SANDU, A.V., Rev. Chim. (Bucharest), **68,** no. 2, 2017, p. 265.

12.NABIALEK, M., PIETRUSIEWICZ, P., SZOTA, M., ABDULLAH, M.M.A., SANDU, A.V., Rev. Chim. (Bucharest), **68,** no. 1, 2017, p. 22.

13.JEZ, B., NABIALEK, M., PIETRUSIEWICZ, P., GRUSZKA, K., BLOCH, K., GONDRO, J., RZACKI, J., ABDULLAH, M.M.A.B., SANDU, A.V., SZOTA, M., JEZ, K., SALAGACKI, A., IOP Conference Series-Materials Science and Engineering, Volume: 209, 2017, Article Number: UNSP 012023. DOI: 10.1088/1757-899X/209/1/012023

14.VLAD, L., SANDU, A.V., GEORGESCU, V., Journal of Superconductivity and Novel Magnetism, **25,** no. 2, 2012, p. 469. DOI: 10.1007/s10948-011-1301-7

15.PINZARU, D., TANASE, S.I., PASCARIU, P., SANDU, A.V., NICA, V., GEORGESCU, V., Optoelectronics and Advanced Materials-Rapid Communications, **5,** no. 3-4, 2011, p. 235.

16.TOTH, L., HARASZTI, F., KOVACS, T., European Journal of Materials Science and Engineering, 3, no. 2, 2018, p. 98.

17.HAN, Y., KONG, F.L., HAN, F.F., INOUE, A., ZHU, S.L., SHALAAN, E., AL-MARZOUKI, F., Intermetallics, **76**, 2016, p. 18.

18.WANG, F., INOUE, A., HAN, Y., ZHU, S.L., KONG, F.L., ZANAEVA, E., LIU, G.D., SHALAAN, E., AL-MARZOUKI, F., OBAID, A., Journal of Alloys and Compounds, **723**, 2017, p. 376.

19.ROY, R.K., PANDA, A.K., MITRA, A., Journal of Magnetism and Magnetic Materials **418**, 2016, p. 236.

20.JEZ, B., Rev.Chim. (Bucharest), **68**, no. 8, 2017, p. 1903.

21.BLOCH, K., NABIALEK, M., Acta Physica Polonica A, **127**, 2015, p. 442.

22.KRONMULLER, H., FAHNLE, M. GRIMM, H., GRIMM, R., GROGER, B., J. Magn. Magn. Mater., **13**, 1979, p. 53.

23.KRONMULLER, H., IEEE Trans. Magn., **15**, 1979, p. 1218.

24.KRONMULLER, H., General Micromagnetic Theory, Handbook of Magnetism and Advanced Magnetic Materials, John Wiley&Sons Vol 2, 2007, p. 703-739.

25.HOLSTEIN, T., PRIMAKOFF, H., Phys. Rev., 58, 1940, p. 1098.

26.LIEBERMANN, H., Rapidly Solidified Alloys, Springer, New Jersey 1993.

27.NABIALEK, M., Journal of Alloys and Compounds, **645**, 2015, p. 98.

Manuscript received: 3.03.2018